The Company of **Biologists**

RESEARCH ARTICLE

The homotetramerization of a GPCR transmits the 20-hydroxyecdysone signal and increases its entry into cells for insect metamorphosis

Xin-Le Kang, Yan-Xue Li, Yan-Li Li, Jin-Xing Wang and Xiao-Fan Zhao*

ABSTRACT

Animal steroid hormones initiate signaling by passive diffusion into cells and binding to their nuclear receptors to regulate gene expression. Animal steroid hormones can initiate signaling via G protein-coupled receptors (GPCRs); however, the underlying mechanisms are unclear. Here, we show that a newly discovered ecdysone-responsive GPCR, ErGPCR-3, transmits the steroid hormone 20-hydroxyecdysone (20E) signal by binding 20E and promoting its entry into cells in the lepidopteran insect *Helicoverpa armigera*. Knockdown of *ErGPCR-3* in larvae caused delayed and abnormal pupation, inhibited remodeling of the larval midgut and fat body, and repressed 20E-induced gene expression. Also, 20E induced both the interaction of ErGPCR-3 with G proteins and rapid intracellular increase in calcium, cAMP and protein phosphorylation. ErGPCR-3 was endocytosed by GPCR kinase 2-mediated phosphorylation, and interacted with β-arrestin-1 and clathrin, to terminate 20E signaling under 20E induction. We found that 20E bound to ErGPCR-3 and induced the ErGPCR-3 homodimer to form a homotetramer, which increased 20E entry into cells. Our study revealed that homotetrameric ErGPCR-3 functions as a cell membrane receptor and increases 20E diffusion into cells to transmit the 20E signal and promote metamorphosis.

KEY WORDS: GPCR, Homotetramer, Facilitated-diffusion, Steroid hormone receptor, Metamorphosis

INTRODUCTION

In mammals, estrogen binds to its nuclear estrogen receptors (ERα and ERβ) to regulate gene transcription (Dahlman-Wright et al., 2006). However, a G protein-coupled receptor (GPCR), GPR30/GPER, was identified as a cell membrane receptor for estrogen (Revankar et al., 2005). Similarly, in insects, the steroid hormone 20-hydroxyecdysone (20E) binds to the nuclear receptor (ecdysone receptor, EcR) to form a transcription complex with their heterodimeric partner ultraspiracle (USP) to initiate gene transcription (Riddiford et al., 2000). However, 20E also triggers a rapid intracellular Ca^{2+} increase via GPCRs in the *Bombyx mori* anterior silk gland (Manaboon et al., 2009). A GPCR, dopamine/ ecdysteroid receptor (DopEcR), is considered as a 20E cell membrane receptor because it binds 20E to regulate non-genomic

effects of ecdysteroids in *Drosophila melanogaster* (Srivastava et al., 2005). Two GPCRs, ecdysone responsive (Er)GPCR-1 (Cai et al., 2014) and ErGPCR-2 (Wang et al., 2015) transmit the 20E signal via the nongenomic pathway in *Helicoverpa armigera*. ErGPCR-2 and DopEcR from *H. armigera* can bind 20E and function as 20E cell membrane receptors (Kang et al., 2019). Therefore, multiple GPCRs are likely to function as 20E receptors; however, whether any other GPCRs function in the 20E pathway and their associated mechanisms is unknown.

GPCRs can form homo- or hetero-oligomers to exert their functions (Cheng et al., 2003; Cheng and Miller, 2001). For example, a family B GPCR is present as a constitutive homodimer in the plasma membrane of pancreatic cancer cell lines (Ding et al., 2002). Oligomerization of GPCRs can be constitutive or ligand-dependent (Ding et al., 2002; Kroeger et al., 2001; Pfleger and Eidne, 2005). However, whether a GPCR functions as an oligomer in steroid hormone signaling, and the regulatory mechanism and outcomes, remain unclear.

Animal steroid hormones are lipophilic hormones that enter cells by passive diffusion across the plasma membrane (Gorski and Gannon, 1976; Plagemann and Erbe, 1976). However, some studies have suggested that steroid hormones require protein transporters for their cellular entry (Milgrom et al., 1973; Pietras and Szego, 1977). Ecdysteroid is imported into cells by a transporter, Ecdysone Importer (EcI), instead of by passive diffusion in *D. melanogaster* (Okamoto et al., 2018). Our previous work has shown that a GPCR, ErGPCR-2, controls 20E entry into cells in *H. armigera* (Wang et al., 2015); however, the mechanism and outcomes are unclear.

In the present study, a new ecdysone-responsive GPCR in *H. armigera*, named ErGPCR-3, was identified as a cell membrane receptor of 20E that transmits the 20E signal and promotes metamorphosis. ErGPCR-3 could bind 20E in the cell membrane and after being isolated from the cell membrane. 20E binding induced homotetramerization of ErGPCR-3. The ErGPCR-3 homotetramer transmits 20E signaling, and increases the entry of 20E into cells. This is the first example of a GPCR functioning as a homotetramer in steroid hormone signaling, and it increases our understanding of GPCR-mediated 20E signaling and supports the facilitated diffusion model of steroid hormones in lepidopterans.

RESULTS

ErGPCR-3 was screened and shown to be upregulated by 20E

Thirteen genes encoding GPCRs, which were identified from the transcriptome of the *H. armigera* epidermal cell line (HaEpi), were examined in the sixth instar 24 h larval epidermis using quantitative real-time reverse transcription PCR (qRT-PCR) under 20E induction (500 ng/larva) for 20 h to screen for 20E-upregulated GPCRs. Six GPCR genes (*GPCR-3*, *-49*, *-24*, *-5*, *-55* and *-56*) were

DEVELOPMENT

1

upregulated by 20E induction, in which *HR3* was used as a positive control and dimethyl sulfoxide (DMSO) was the solvent control (Fig. S1A). The six 20E-upregulated GPCR genes were knocked down by injecting double-stranded RNA (dsRNA) into the *H. armigera* sixth instar 6 h larval hemocoel to identify the GPCRs that are involved in 20E-directed gene expression. 20E induced the expression of ecdysone nuclear receptor *EcRB1*, the heterodimeric partner *USP1*, and transcription factors *HR3* and *BrZ7* in the epidermis; however, knockdown of *ErGPCR-3* repressed these functions of 20E compared with knockdown of the other GPCR genes (Fig. S1B-G), suggesting that *ErGPCR-3* plays a role in the 20E pathway. Phylogenetic analysis indicated that *H. armigera* ErGPCR-3 (MN150685) and its orthologs in insects are class B receptors (Secretin receptor Mth2-like) (Fig. S2).

To study the function of ErGPCR-3 in *H. armigera* development, the developmental expression profiles and hormonal regulation of ErGPCR-3 were examined. ErGPCR-3 was expressed in the epidermis, midgut and fat body. The protein levels of ErGPCR-3 increased at the fifth instar molting (5 M) and metamorphic stages (sixth instar 72 h to 120 h) compared with the 5th instar feeding larvae (5 F), as assessed using western blotting with rabbit polyclonal antibodies recognizing ErGPCR-3 (Fig. 1A,A′). The expression of ErGPCR-3 in the epidermis was increased by 20E injection into the sixth instar 6 h larvae (Fig. 1B,B′). ErGPCR-3 expression was proven to be upregulated by 20E via the EcRB1-USP1 transcription complex via knockdown of *EcRB1* and *USP1* in

HaEpi cells, the identification of an ecdysone response element (EcRE)-containing sequence (5′-56-GCGTTCATAGAACTT-42-3′ before the ATG codon) in the 5′-upstream genomic DNA region of *ErGPCR-3*, and using chromatin immunoprecipitation (ChIP) (Fig. S3). Immunohistochemistry showed that ErGPCR-3 was abundant and localized in the larval midgut of sixth instar 96 h larvae (Fig. 1C), suggesting that ErGPCR-3 might play an important role in the 20E pathway.

ErGPCR-3 knockdown repressed 20E-induced pupation, tissue remodeling and gene expression

To examine the function of ErGPCR-3 in 20E-regulated metamorphosis, we knocked down *ErGPCR-3* via injection of *dsErGPCR-3* into sixth instar 6 h larvae. 20E promotes earlier pupation; however, after knockdown of *ErGPCR-3*, 20E did not promote pupation, but appeared to cause pupation delay, pupation failure and emergence failure, compared with larvae injected with *dsGFP* plus 20E (Fig. 2A,B). 20E injection accelerated the initiation time of pupation to 28 h on average. However, 20E could not accelerate pupation after injection of *dsErGPCR-3* plus 20E, and pupation time was delayed by 38 h compared with that in larvae injected with *dsGFP* plus 20E injection (Fig. 2C). In the animals showing delayed pupation after *dsErGPCR-3* plus 20E treatment, the rates of normal pupation, pupation failure and emergence failure were 43%, 26% and 21%, respectively (Fig. 2D). After *ErGPCR-3* was significantly knocked down in the midgut, 20E could not
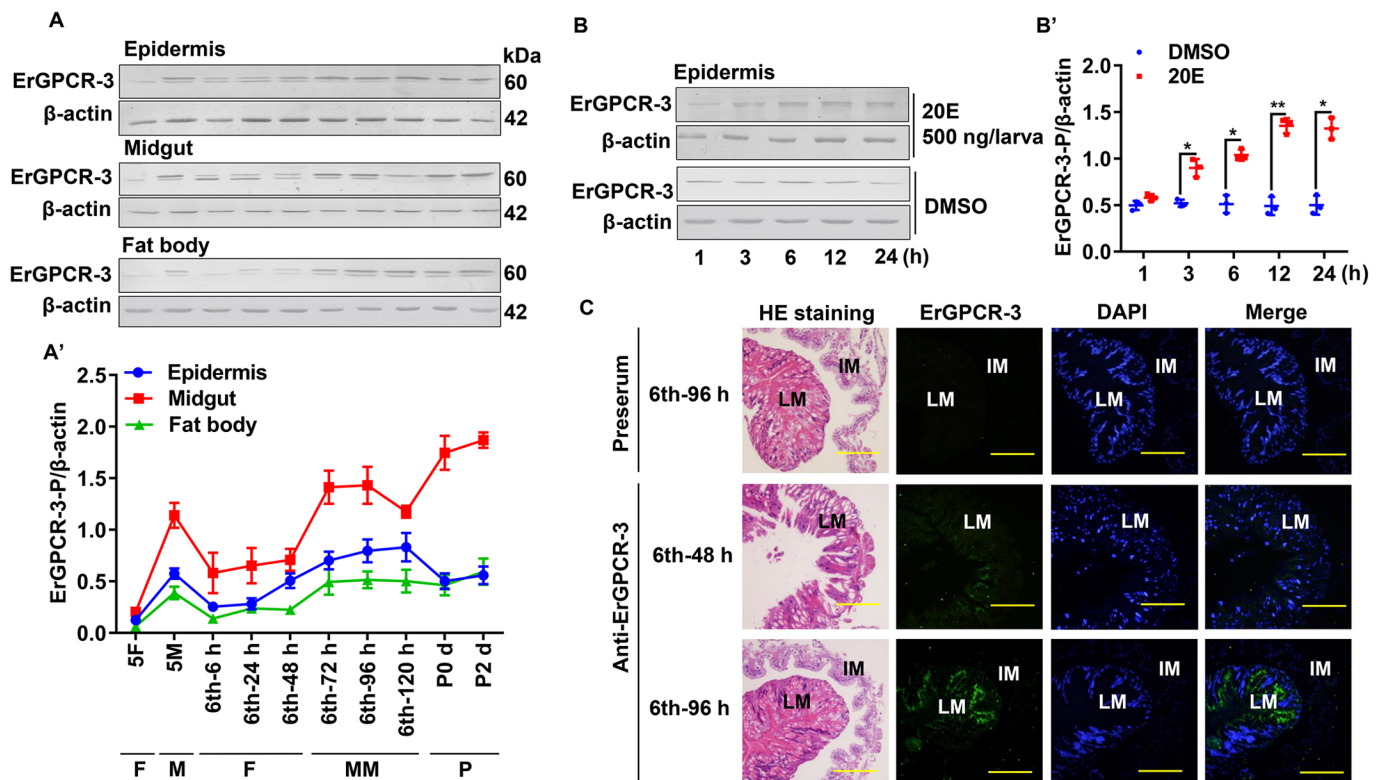
Fig. 1. ErGPCR-3 levels increased during metamorphosis. (A,A′) Western blot (A) and quantification (A′) of expression profiles of ErGPCR-3 detected by anti-ErGPCR-3 polyclonal antibodies. β-Actin was detected by the antibodies as the protein quality control. SDS-PAGE gel in western blotting is 7.5%. (B,B′) Western blot (B) and quantification (B′) showing 20E regulation on ErGPCR-3 expression (500 ng/larva at sixth instar 6 h). An equal volume of DMSO was injected as a control. Data are mean±s.d. of three replicates. *$P<0.05$, **$P<0.01$ (two-tailed Student's t-test). (C) ErGPCR-3 localization in the larval midgut during metamorphosis by immunohistochemical analysis. The pre-serum was used as negative control. H&E staining shows the morphology of the midgut: green fluorescence indicates ErGPCR-3; nuclei were stained with DAPI (blue). 5F, 5th instar feeding larvae; 5M, 5th instar molting larvae; F, feeding stage; IM, imaginal midgut; LM, larval midgut; M, molting stage; MM, metamorphic molting stage; P, pupae; sixth-6 h, sixth instar at 6 h larvae; sixth-24 h to sixth-120 h, sixth instar 24 h larvae to sixth instar 120 h larvae; P0 d to P2 d: pupal stage at 0 day to pupal stage at 2 day. Scale bars: 100 μm.
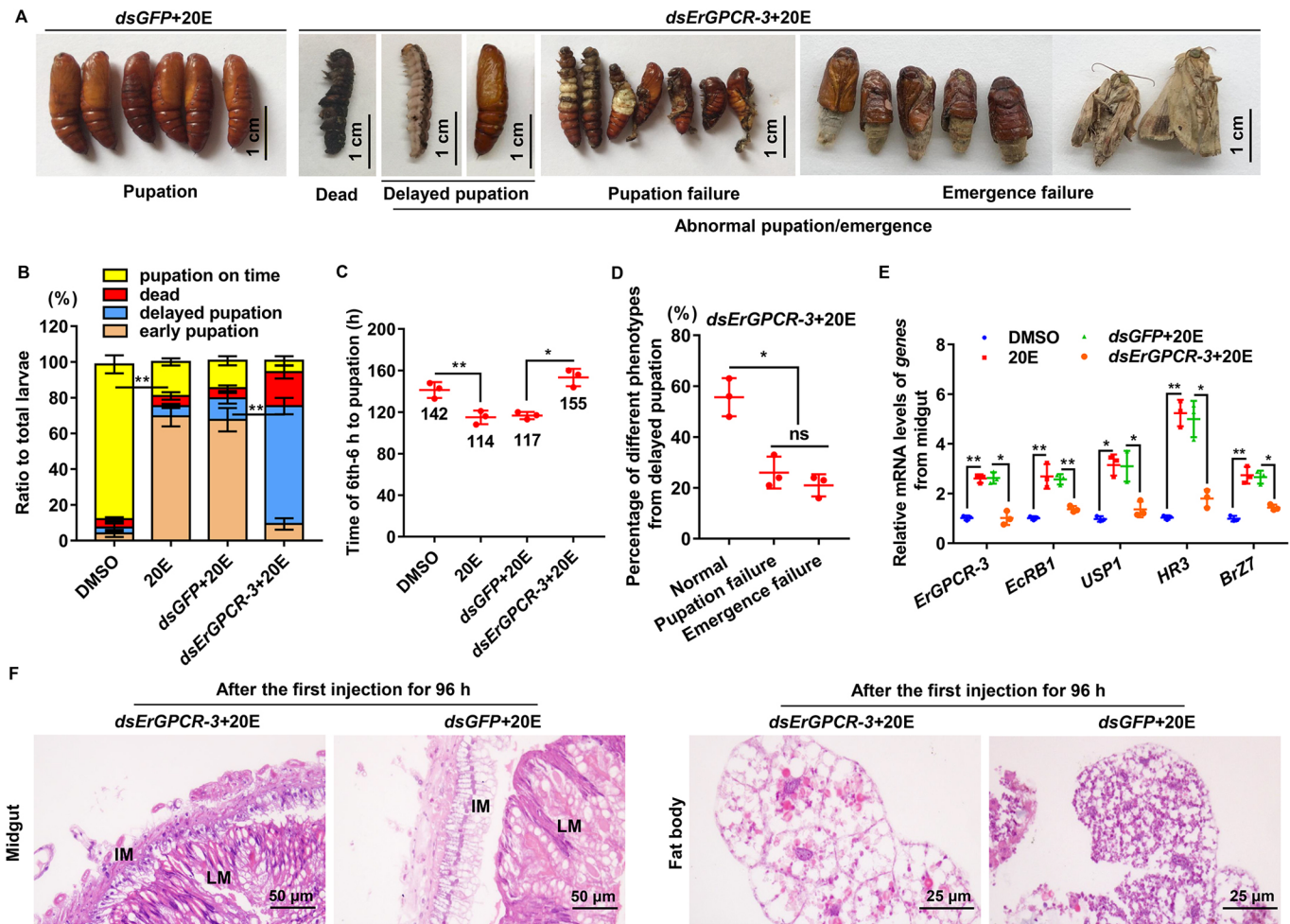
Fig. 2. dsRNA injection-induced knockdown of *ErGPCR-3* delayed pupation. (A) Phenotypes after *ErGPCR-3* knockdown (500 ng/larva at sixth instar 6 h, thrice at an 18 h interval) and 20E treatment (500 ng/larva) at the third injection. Images were obtained at six instar larvae 120 h, pupal stage at day 2 and adult stage at day 2 according to the DMSO control group. (B) Quantification of the phenotype in A. (C) Statistical analysis of pupation time from sixth instar 0 h larvae to pupae. The data were calculated from 30 larvae×3 experiments. (D) Percentage of different phenotypes from delayed-pupation. (E) qRT-PCR showing the mRNA levels of 20E response genes after *ErGPCR-3* knockdown in larvae at sixth instar 72 h larvae. (F) H&E-stained midgut (left) and fat body (right) after knockdown of *ErGPCR-3*. *dsGFP* was used as a control. IM, imaginal midgut; LM, larval midgut. Data are mean±s.d. of three replicates. *P<0.05, **P<0.01 (two-tailed Student's *t*-test).

upregulate the expression of the key genes in the 20E pathway, including *EcRB1*, *USP1*, *HR3* and *BrZ7* (Fig. 2E). Hematoxylin and Eosin (H&E) staining showed that the larval midgut did not separate from imaginal midgut after the first injection of *dsErGPCR-3* plus 20E for 96 h, compared with the larvae injected with the control *dsGFP* plus 20E for 96 h. The fat bodies of the *dsErGPCR-3* plus 20E-treated larvae were still closely arranged; however, the *dsGFP* plus 20E control larvae showed initial fat body degradation (Fig. 2F). These results suggest that ErGPCR-3 participates in 20E-regulated metamorphosis and tissue remodeling.

dsRNA-mediated knockdown of *ErGPCR-3* was performed in sixth instar larvae to determine further the function of *ErGPCR-3* during *H. armigera* growth and metamorphosis. Compared with that in the *dsGFP* injection control group, the larvae injected with *dsErGPCR-3* showed abnormal pupation, pupation delay and pupation failure (Fig. S4A,B). The pupation of the *dsErGPCR-3* injection group was delayed by about 29 h on average (recorded from sixth instar 0 h) compared with that in the *dsGFP* injection control group (Fig. S4C). The mRNA levels of *EcRB1*, *USP1*, *HR3*

and *BrZ7* were downregulated after *ErGPCR-3* was significantly knocked down in the midgut (Fig. S4D). The efficiency of RNAi of ErGPCR-3 was confirmed by western blotting (Fig. S4E). The midgut did not turn red after injection of *dsErGPCR-3* for 96 h and the larval midgut did not separate from the imaginal midgut compared with the larvae injected with the control *dsGFP* injection. Similarly, the fat body of the *dsGFP* control larvae showed initial degradation, whereas the fat body of the *dsErGPCR-3*-treated larvae was still closely arranged (Fig. S4F-H). These results suggest that ErGPCR-3 is necessary for metamorphosis.

ErGPCR-3 participated in 20E-induced rapid cellular reactions via interacting with Gαq and Gαs

The involvement of ErGPCR-3 in 20E-induced Ca^{2+} influx and intracellular cAMP levels was detected in HaEpi cells to address its role in 20E signaling. 20E induced the rapid release of intracellular Ca^{2+} and extracellular Ca^{2+} influx. However, *ErGPCR-3* knockdown (the RNAi efficiency of *ErGPCR-3* is shown in Fig. S5A) decreased the 20E-induced Ca^{2+} release and influx (Fig. 3A). Similarly, the 20E-induced increase in cAMP levels was decreased
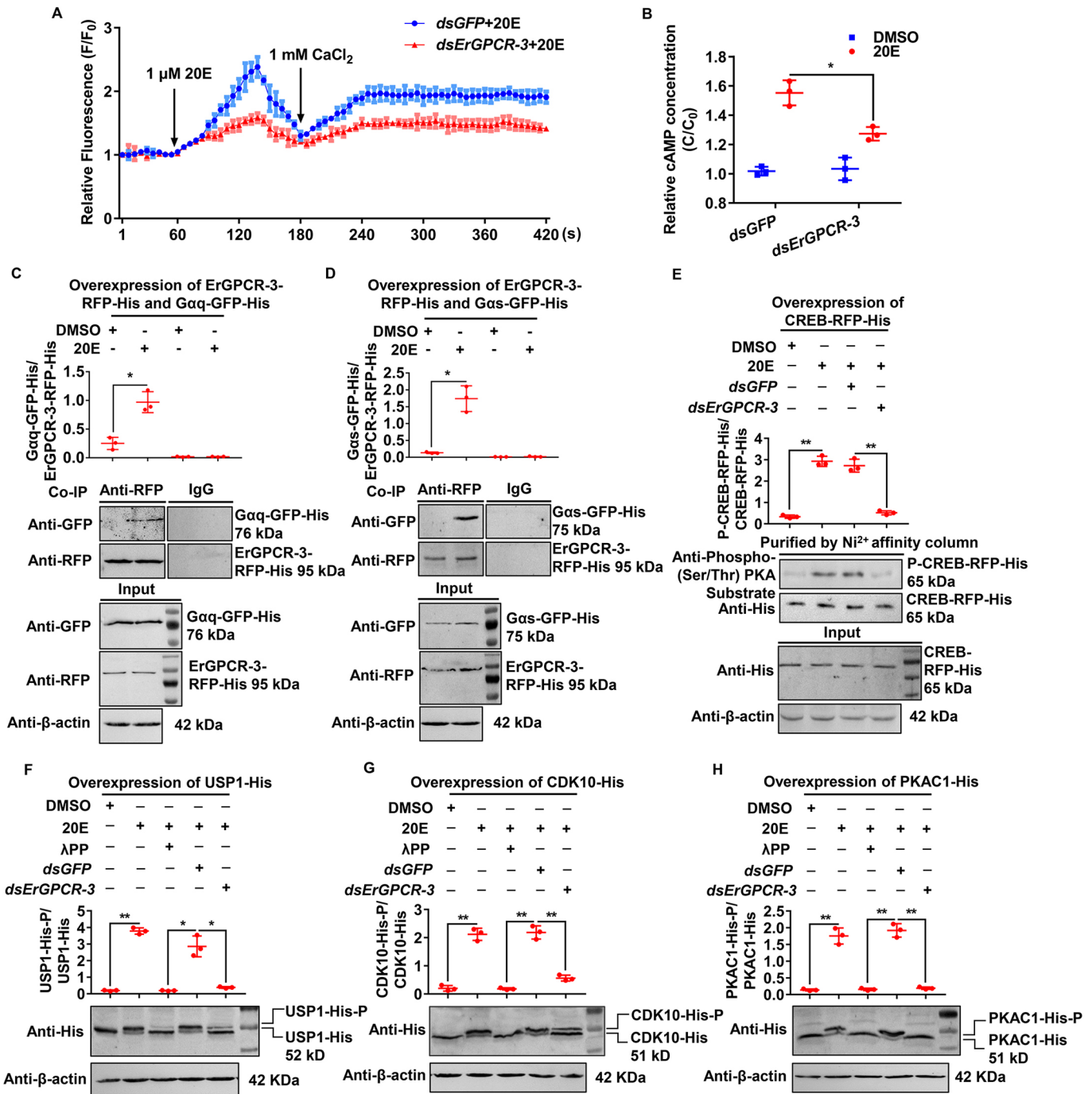
Fig. 3. ErGPCR-3 participated in 20E-induced rapid cellular reaction and protein phosphorylation. (A) Ca^{2+} levels after *ErGPCR-3* knockdown in HaEpi cells. *dsGFP* or *dsErGPCR-3* (1 μg/ml in the medium) for 48 h. AM ester calcium crimson dye (3 μM) in DPBS for 30 min. F, fluorescence intensity of HaEpi cells after different treatments; F$_0$, fluorescence intensity before different treatments. (B) cAMP levels after *ErGPCR-3* knockdown in HaEpi cells. *dsErGPCR-3* or *dsGFP* (1 μg/ml) for 48 h, 20E (2 μM). (C,D) ErGPCR-3 coupling with Gαq (C) and Gαs (D) under 20E induction (2 μM for 30 min). DMSO was solvent control. Input: the levels of Gαq-GFP-His, ErGPCR-3-RFP-His and Gαs-GFP-His in the cells detected by an antibody against GFP or RFP. β-Actin was a loading control. Co-IP: Anti-RFP antibody co-immunoprecipitated ErGPCR-3-RFP-His. Nonspecific mouse IgG was a negative control. 12.5% gel in SDS-PAGE. (E) 20E via ErGPCR-3 induced CREB phosphorylation (P-CREB-RFP) by the phospho-(Ser/Thr) PKA substrate antibody after CREB-RFP-His was affinity isolated. *dsErGPCR-3* or *dsGFP* (1 μg/ml for 12 h), 20E (2 μM) or DMSO for 0.5 h. Input: the expression levels of CREB-RFP-His in HaEpi cells detected by an antibody against the His tag. (F-H) 20E via ErGPCR-3-induced phosphorylation of USP1-His, CDK10-His and PKAC1-His (2 μM 20E for 0.5 h) using the anti-His antibody. λPP, 0.5 μM λ protein phosphates incubation. 7.5% SDS-PAGE gel. Data are mean±s.d. of three replicates. *$P<0.05$, **$P<0.01$ (two-tailed Student's *t*-test).

after *ErGPCR-3* knockdown (Fig. 3B). These data suggest that ErGPCR-3 participates in the 20E-induced rapid cellular responses.

GPCRs transmit extracellular signals by activating different heterotrimeric G proteins (Bockaert and Pin, 1999). The s and q subunits of Gα stimulate the effector molecules adenylyl cyclase (AC) and phospholipase C (PLC), thereby increasing the intracellular concentration of cAMP and Ca^{2+}, respectively (Marinissen and Gutkind, 2001). To address the mechanism by which 20E increases

intracellular Ca^{2+} and cAMP levels via ErGPCR-3, the protein interactions between ErGPCR-3 and Gαq or Gαs were examined by co-overexpression of ErGPCR-3-RFP-His and either Gαq-GFP-His or Gαs-GFP-His in HaEpi cells, followed by co-immunoprecipitation (Co-IP) via the fused tags. Gαq-GFP-His was co-immunoprecipitated with ErGPCR-3-RFP-His in 20E-induced cells using the anti-RFP antibody when they were co-expressed in cells (Input), compared with the negative IgG control (Fig. 3C). Similarly, Gαs-GFP-His was co-immunoprecipitated with ErGPCR-3-RFP-His using the anti-RFP antibody in 20E-induced cells (Fig. 3D). These data suggest that ErGPCR-3 transmits signals via Gαs and Gαq.

20E induces rapid protein phosphorylation, including that of cAMP response element-binding (CREB) and protein kinase A catalytic subunit 1 (PKAC1) via cAMP signaling (Jing et al., 2016), and USP1 (Liu et al., 2014b) and cyclin dependent kinase 10 (CDK10) (Liu et al., 2014a) via calcium signaling. Therefore, to address the involvement of ErGPCR-3 in 20E-induced protein phosphorylation, we co-overexpressed these four proteins (with tags for antibody recognition), with or without *ErGPCR-3* knockdown. 20E induced the phosphorylation of these proteins; however, knockdown of *ErGPCR-3* repressed the 20E-induced phosphorylation of the four proteins (Fig. 3E-H). These data suggest that ErGPCR-3 participates in 20E-induced rapid protein phosphorylation.

20E induced ErGPCR-3 phosphorylation and internalization
To clarify the response of ErGPCR-3 to 20E, the phosphorylation and subcellular location of ErGPCR-3 were analyzed. ErGPCR-3 was internalized into the cytoplasm after 20E treatment for 15 min, and the findings compared with those in the DMSO treatment control (Fig. 4A). Western blotting analysis showed that the molecular mass of the internalized protein was higher than that in the cell membrane, and lambda protein phosphatase (λPPase) treatment decreased the apparent molecular mass (Fig. 4A′), suggesting that 20E induced ErGPCR-3 phosphorylation and internalization.

G protein-coupled receptor kinases (GRKs) deactivate GPCR signaling by phosphorylating the C-terminus of the receptor (He et al., 2017; Wang et al., 2015). To identify the relationship between the phosphorylation and internalization of ErGPCR-3, ErGPCR-3-GFP and a C-terminal deletion (amino acids 479-534) of ErGPCR-3 (ErGPCR-3$^{\Delta C-terminal}$-GFP) were overexpressed in HaEpi cells, and GFP was overexpressed as a control. GFP was detected throughout the cell. ErGPCR-3-GFP-His appeared in the cell membrane under DMSO treatment, and was internalized by 20E induction; however, ErGPCR-3$^{\Delta C-terminal}$-GFP-His remained in the cell membrane under both DMSO and 20E treatment (Fig. 4B). Western blotting showed that ErGPCR-3-GFP-His was phosphorylated after 20E induction; however, ErGPCR-3$^{\Delta C-terminal}$-GFP-His remained unphosphorylated after 20E induction (Fig. 4B′). These results suggest that 20E-induced phosphorylation of the C-terminus of ErGPCR-3 determines the internalization of ErGPCR-3.

GPCR internalization is regulated by GRK phosphorylation, which promotes its interaction with β-arrestin (Benovic et al., 1989; Lohse et al., 1990). Clathrin participates in GPCR endocytosis (Chen et al., 2014) and chlorpromazine (CPZ) inhibits the recirculation of clathrin to the plasma membrane, thereby inhibiting clathrin-mediated endocytosis (Bhattacharyya et al., 2010). Therefore, the internalization of ErGPCR-3 was examined by knockdown of the genes encoding these proteins or by inhibiting clathrin using its inhibitor CPZ to address the mechanism of ErGPCR-3 internalization. Immunocytochemical analysis showed that ErGPCR-3 was internalized after 15 min of 20E induction in

the *dsGFP* control cells. However, ErGPCR-3 was not internalized in the *dsGRK2*, *dsβ-arrestin-1* (the RNAi efficiency of *GRK2* and *β-arrestin-1* are shown in Fig. S5B,C), or CPZ-treated cells (Fig. 4C), suggesting that ErGPCR-3 was internalized by 20E via GRK2, β-arrestin-1 and clathrin. Western blotting analysis further confirmed that ErGPCR-3 was phosphorylated and internalized into the cytoplasm by 20E induction in the *dsGFP* control cells; however, ErGPCR-3 was not phosphorylated or internalized by 20E induction after knockdown of *GRK2* or *β-arrestin-1*, or CPZ treatment (Fig. 4C′), suggesting that 20E induced ErGPCR-3 phosphorylation and internalization via GRK2, β-arrestin-1 and clathrin.

Co-IP using the anti-RFP antibody further showed that β-arrestin-1-GFP-His could be co-immunoprecipitated together with ErGPCR-3-RFP-His under 20E induction, when they were co-overexpressed in the cells (Fig. 4D). Similarly, GRK2-GFP-His was co-immunoprecipitated with ErGPCR-3-RFP-His (Fig. 4E). These results suggest that 20E induces the internalization of ErGPCR-3 via GRK2 and β-arrestin-1.

Chloroquine (CQ; Sangon Biotech), a lysosome inhibitor (Gonzalez-Noriega et al., 1980), was used to analyze the fate of ErGPCR-3 in cells. ErGPCR-3 was localized in the cell membrane in the DMSO control, but localized in the cytoplasm after 20E induction. After the withdrawal of 20E, ErGPCR-3 levels decreased in the cytoplasm; however, ErGPCR-3 accumulated in the cytoplasm after the addition of CQ. The subcellular localization and degradation of ErGPCR-3 were not well observed in cells (Fig. 4F); however, western blotting after subcellular fractionation showed that ErGPCR-3 was localized in the cell membrane in the DMSO control and was internalized into the cytoplasm by 20E. The level of ErGPCR-3 in the cytoplasm decreased after the removal of 20E for 2 h in CQ-free medium. However, the level of ErGPCR-3 in the cytoplasm was maintained after removing 20E in the presence of CQ (Fig. 4F′). These results suggest that ErGPCR-3 is degraded in the lysosome after internalization.

ErGPCR-3 bound 20E
To determine whether ErGPCR-3 is a 20E receptor, a binding experiment was performed. Surflex-Dock (SFXC) in the SYBYL X 2.0 software was used to conduct a computational docking of 20E to ErGPCR-3. The model showed that 20E bound ErGPCR-3 near the transmembrane helix. 20E formed two hydrogen bonds with residues M240 and L331 of ErGPCR-3 (Fig. 5A). To prove that ErGPCR-3 binds 20E, ErGPCR-3-GFP and its mutant ErGPCR-3-M-GFP (with mutations of the 20E binding sites of ErGPCR-3-GFP; Table S2) were overexpressed in Sf9 cells. GFP in the control was distributed throughout the whole cell, and both ErGPCR-3-GFP and its mutant ErGPCR-3-M-GFP were localized in the cell membrane, with wheat germ agglutinin (WGA) staining indicating the cell membrane (Fig. 5B). A binding assay using 20E Enzyme Immunoassay (20E-EIA) showed that the amount of cell membrane-bound 20E in ErGPCR-3-GFP-overexpressing cells was significantly higher than that in ErGPCR-3-M-GFP- and GFP-overexpressing control cells (Fig. 5C). These results showed that ErGPCR-3 could bind 20E in the cell membrane.

The dissociation constant (Kd) of ErGPCR-3 binding 20E was further determined using a saturation binding curve detected using the 20E-EIA method with isolated ErGPCR-3. The purity of the isolated GFP, ErGPCR-3-GFP and ErGPCR-3-M-GFP was examined using sodium dodecylsulfate polyacrylamide gel electrophoresis (SDS-PAGE) with Coomassie Brilliant Blue staining (Fig. S6). The saturable specific binding of ErGPCR-3-
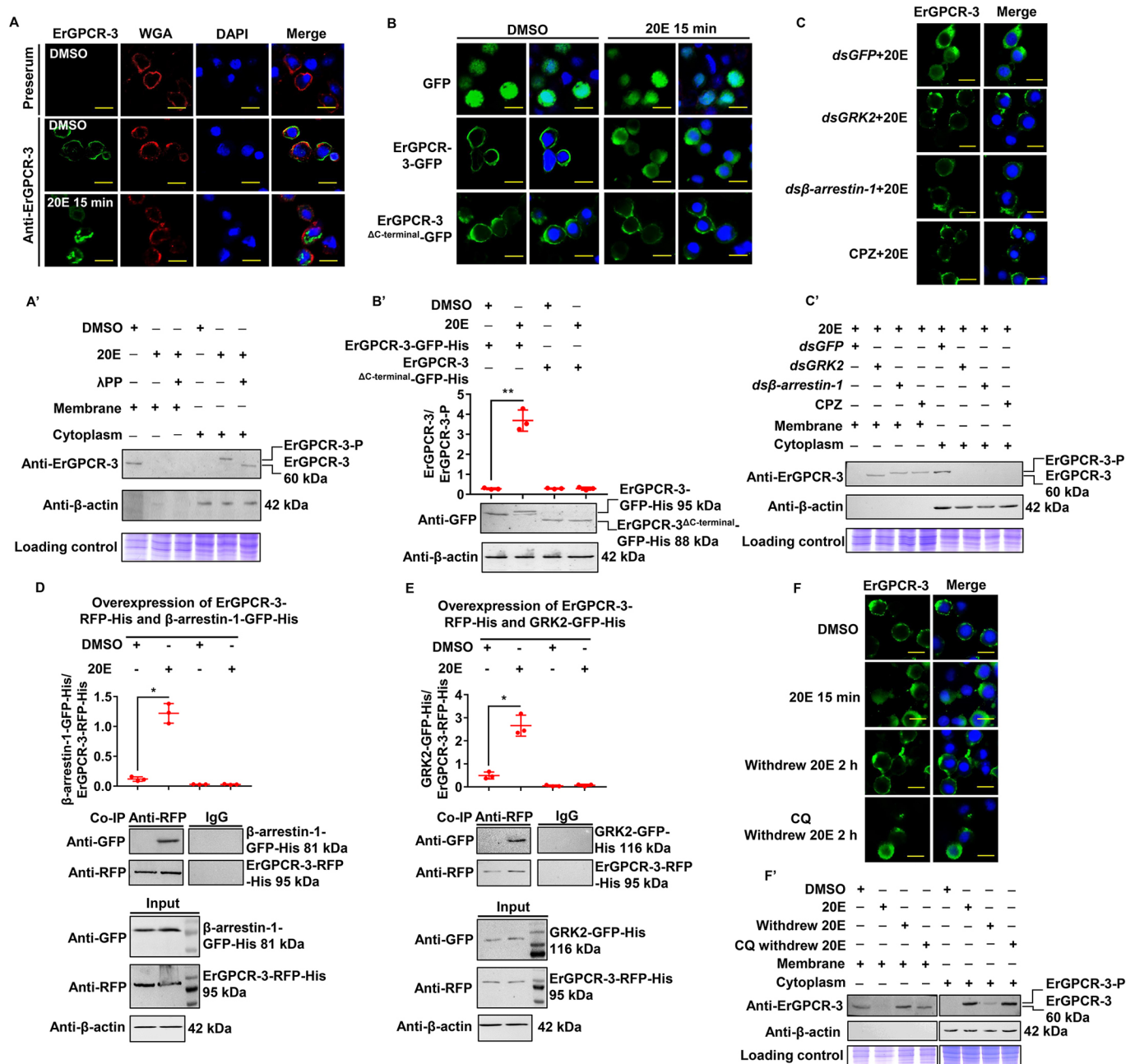
Fig. 4. 20E regulated the phosphorylation of ErGPCR-3 and its internalization in HaEpi cells. (A) Localization of ErGPCR-3 in HaEpi cells. Green shows ErGPCR-3 protein stained with an anti-ErGPCR-3 and secondary antibody labeled with Alexa Fluor 488. Red shows plasma membrane stained with Alexa Fluor 594-conjugated wheat germ agglutinin (WGA). Blue shows nuclei stained with DAPI. (A′) Western blotting showing the subcellular distribution and phosphorylation of ErGPCR-3. Gel concentration of SDS-PAGE is 7.5%. β-Actin and Coomassie Brilliant Blue staining were used as a loading control for cytoplasm or membrane protein quantity and quality, respectively. λPP, λ protein phosphates. (B) Overexpression of ErGPCR-3-GFP and its mutant ErGPCR-3^{ΔC−terminal}-GFP in HaEpi cells. Green, GFP; blue, nuclei. (B′) Western blotting showing the variation of the phosphorylation of ErGPCR-3 and ErGPCR-3^{ΔC−terminal}-GFP. Gel concentration of SDS-PAGE is 7.5%. (C) HaEpi Cells were treated with *dsGFP, dsGRK2, dsβ-arrestin-1* for 48 h, and CPZ (50 μM) for 2 h, followed by 1 μM 20E for 15 min. Green, ErGPCR-3; blue, nuclei. (C′) Western blotting of the samples in C. β-Actin and Coomassie Brilliant Blue staining are the same as those in A′. (D,E) ErGPCR-3 coupling with β-arrestin-1 and GRK2 under 20E induction (2 μM for 15 min). DMSO was solvent control. Input: the levels of β-arrestin-1-GFP-His, ErGPCR-3-RFP-His and GRK2-GFP-His in the cells detected by an antibody against GFP or RFP. β-Actin was a loading control. Co-IP: anti-RFP antibody co-immunoprecipitated ErGPCR-3-RFP-His and β-arrestin-1-GFP-His or GRK2-GFP-His. Nonspecific mouse IgG was a negative control. SDS-PAGE gel was 12.5%. (F) Degradation of ErGPCR-3 in cytoplasm. DMSO, solvent control for 15 min; 20E, 2 μM for 15 min; withdrew 20E 2 h, withdrew 20E and cultured 2 h; CQ withdrew 20E 2 h, withdrew 20E and cultured with chloroquine (25 μM) for 2 h. Green, ErGPCR-3; blue, nuclei. (F′) Western blotting showing the relative levels of ErGPCR-3 in membrane and cytoplasm after the treatments in F. Data are mean±s.d. of three replicates. *P<0.05, **P<0.01 (two-tailed Student's t-test). Scale bars: 25 μm.

GFP to 20E had a Bmax=9.06±0.43 pmol/mg protein and a Kd= 20.84±2.28 nM (mean±s.d.). However, ErGPCR-3-M-GFP decreased the saturable specific binding, with a Bmax=8.69±1.47 pmol/mg protein and a Kd=84.68±21.23 nM. GFP showed lower binding to 20E (Fig. 5D). The smaller the Kd value, the stronger the binding ability. The 20E-EIA assay was based on competition between the unlabeled
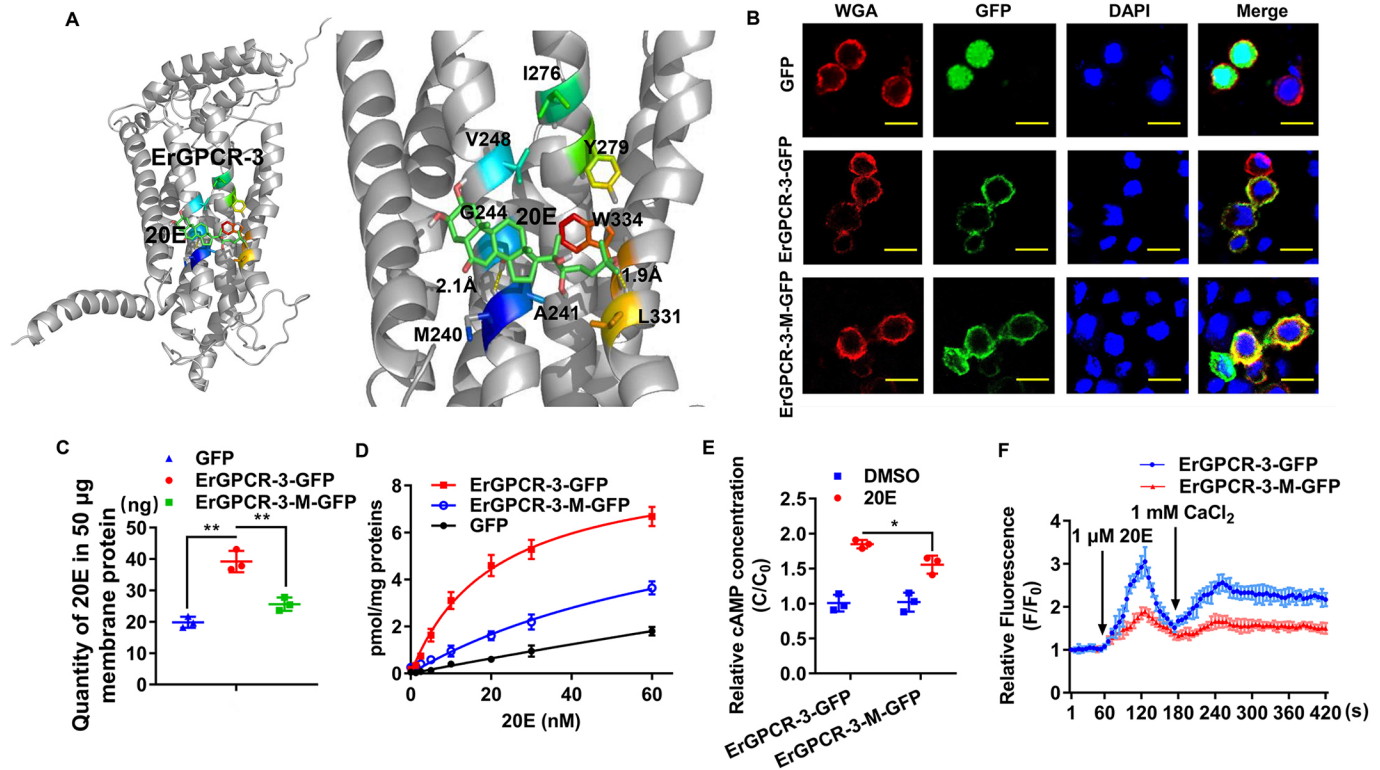
Fig. 5. ErGPCR-3 could bind 20E. (A) Modeling of the ligand-binding complex of the ErGPCR-3 predicted by software. ErGPCR-3, gray: 20E, green. The dotted lines indicate the predicted hydrogen bonds between the amino acid residues and 20E. The residues that interact with the 20E are represented as sticks with different colors. The predicted binding residues and point mutations are in Table S2. (B) HaEpi cell membrane localization of the overexpressed GFP, ErGPCR-3-GFP and ErGPCR-3-M-GFP. The cell membrane was marked by wheat germ agglutinin (WGA; red). GFP, green fluorescence from GFPs, ErGPCR-3-GFP and ErGPCR-3-M-GFP. Blue, nuclei. (C) Quantity of 20E bound by 50 µg membrane protein from HaEpi cells that overexpressed GFP-His, ErGPCR-3-GFP-His and ErGPCR-3-M-GFP-His. (D) Saturation binding curves of ErGPCR-3-GFP and ErGPCR-3-M-GFP to 20E. GFP is a non-specific binding control. All of the experiments were performed using 10 µg of isolated protein in 50 µl EIA buffer. (E,F) Mutation of ErGPCR-3 decreased cAMP and Ca^{2+} levels in HaEpi cells. F, fluorescence intensity of HaEpi cells after different treatments; F_0, fluorescence intensity before different treatments. HaEpi cells overexpressed ErGPCR-3-GFP and ErGPCR-3-M-GFP for 48 h followed by incubation with 2 µM 20E. Data are mean±s.d. of three replicates. *$P<0.05$, **$P<0.01$ (two-tailed Student's t-test). Scale bars: 20 µm.

20E (20E bound to GPCR) and acetylcholinesterase-labeled 20E (Tracer) for the limited-specific rabbit anti-20E antiserum; therefore, an inhibition or competitive curve was not produced. HaEpi cells overexpressing the binding sites mutant, ErGPCR-3-M-GFP, had lower intracellular cAMP levels than those overexpressing ErGPCR-3-GFP under 20E incubation (Fig. 5E). Similarly, ErGPCR-3-M-GFP decreased the 20E-induced Ca^{2+} influx (Fig. 5F). These results suggest that the ErGPCR-3 binds 20E to transmit 20E signaling.

ErGPCR-3 existed as a homodimer and was oligomerized to a homotetramer by 20E induction to increase the entrance of 20E into cells

To address whether ErGPCR-3 functions as a monomer or an oligomer, ErGPCR-3 was overexpressed in HaEpi cells in various combinations, including ErGPCR-3-RFP-His and ErGPCR-3-GFP-His, ErGPCR-3-RFP-His and ErGPCR-1-GFP-His, ErGPCR-3-RFP-His and ErGPCR-2-GFP-His, ErGPCR-3-RFP-His and DopEcR-GFP-His. Co-IP using antibodies recognizing RFP resulted in the Co-IP of ErGPCR-3-GFP-His together with ErGPCR-3-RFP-His in both DMSO-treated cells and 20E-induced cells when they were overexpressed equally as Input, with IgG as the negative control (Fig. 6A), suggesting that ErGPCR-3 existed as a homodimer regardless of 20E induction. In the tag-control, RFP-His and GFP-His were not co-immunoprecipitated

(Fig. 6B). In addition, ErGPCR-1-GFP-His, ErGPCR-2-GFP-His and DopEcR-GFP-His were not co-immunoprecipitated with ErGPCR-3-RFP-His (Fig. S7). These data suggest that ErGPCR-3 exists as a homodimer constitutively.

To confirm the homodimeric nature of ErGPCR-3 *in vivo*, suberic acid bis sodium salt [3-sulfo-N-hydroxysuccinimide ester, bis (sulfosuccinimidyl) suberate, BS3] was used to detect ErGPCR-3 oligomers in the larval epidermis using western blotting according to their molecular mass. BS3 can crosslink the protein molecules when they are associated together to prevent them dissociating during SDS-PAGE sample treatment (Sargiacomo et al., 1995). The endogenous monomer of ErGPCR-3 (60 kDa) was detected in both DMSO- and 20E-treated larval epidermis by western blotting without BS3 treatment. Surprisingly, a homotetramer (~240 kDa) of ErGPCR-3 was detected abundantly in the 20E-treated sample after BS3 treatment. In contrast, the homodimer (~120 kDa) of ErGPCR-3 was detected abundantly in the DMSO treatment control after BS3 treatment, although some homotetramer was detected that was likely formed by 20E *in vivo* (Fig. 6C). These data not only confirm that ErGPCR-3 exists as a homodimer *in vivo*, but also indicate that 20E induces ErGPCR-3 to form a homotetramer.

To address the mechanism of homotetramer formation, we examined the variation of homotetramer levels by overexpressing ErGPCR-3-GFP, ErGPCR-3$^{\Delta C-terminal}$-GFP (truncated mutation of the phosphorylation region at the C terminal) and ErGPCR-3-M-
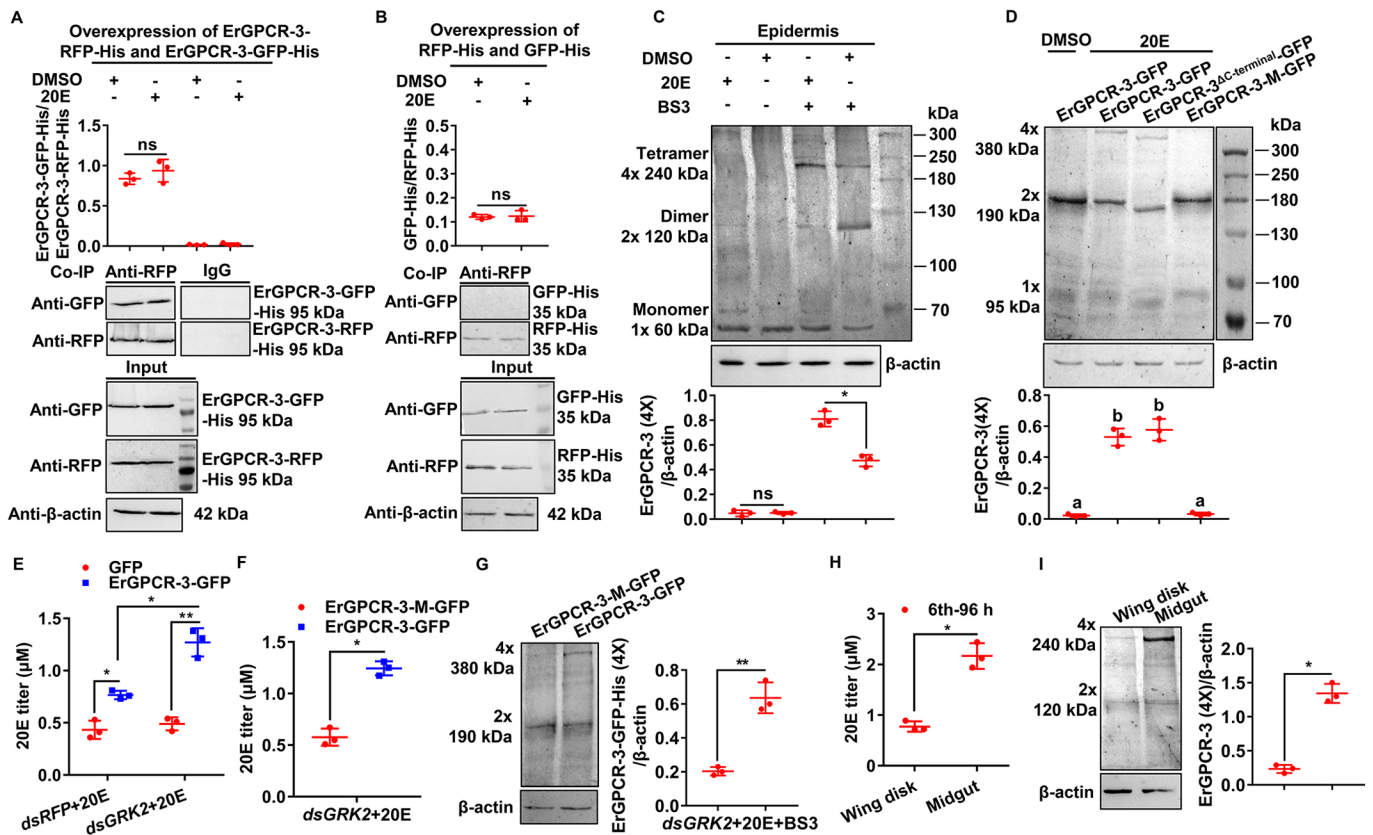
Fig. 6. 20E induced ErGPCR-3 to form a homotetramer in the cell membrane, which increased 20E entry into cells. (A) Co-IP to detect the oligomer of the overexpressed ErGPCR-3 in HaEpi cells. DMSO was solvent control. 20E (2 µM for 30 min). Co-IP: anti-RFP antibody co-immunoprecipitated ErGPCR-3-RFP-His and ErGPCR-3-GFP-His. IgG: nonspecific mouse IgG as a negative control. Input: the levels of ErGPCR-3-GFP-His and ErGPCR-3-RFP-His detected by an antibody against GFP or RFP. β-Actin was a loading control. SDS-PAGE gel was 12.5%. (B) GFP-His and RFP-His as negative tag control for A. (C) Crosslink with BS3 to detect the oligomer of endogenic ErGPCR-3 (60 kDa for monomer) in the larval epidermis using western blotting. 20E (500 ng) was injected into a larva at the sixth instar 6 h. DMSO was control. SDS-PAGE gel was 7.5%. (D) Crosslink with BS3 to detect the variation of the oligomer of ErGPCR-3-GFP (95 kDa for monomer: 60+35 kDa of GFP), ErGPCR-3$^{\Delta C-terminal}$-GFP and ErGPCR-3-M-GFP in HaEpi cells using western blotting. SDS-PAGE gel was 7.5%. HaEpi cells were incubated with 2 µM 20E for 30 min and then treated with BS3. (E) 20E titers in the nuclei of HaEpi cells that overexpress GFP and ErGPCR-3-GFP when ErGPCR-3-GFP was arrested in the cell membrane by knockdown of *GRK2* (*dsRFP* or *dsGRK2* 2 µg/ml for 12 h, twice, followed 20E incubation, 2 µM for 30 min). (F) 20E titers in the nuclei of HaEpi cells that overexpress ErGPCR-3-M-GFP or ErGPCR-3-GFP when they were arrested in the cell membrane by knockdown of *GRK2* as in E. (G) Crosslink with BS3 to show the tetramer of ErGPCR-3-GFP in HaEpi cells after treatment as in F. (H) 20E titers in wing disk and midgut at sixth-96 h larvae. (I) Crosslink with BS3 to show the tetramer of ErGPCR-3 in the wing disk and midgut in sixth-96 h larvae. SDS-PAGE gel was 7.5%. Data are mean±s.d. of three independent biological replicates. For A-C,E-I: *P<0.05, **P<0.01 (two-tailed Student's *t*-test); for D: one-way ANOVA (lower case letters are used to label means, such that bars bearing different letters are statistically different from one another with a minimum *P*-value of <0.05). ns, not significant.

GFP (multiple sites mutation of the 20E binding sites of ErGPCR-3-GFP) in HaEpi cells. Antibodies against GFP were used to detect the oligomers after BS3 treatment. The homodimer (~190 kDa) was detected abundantly in the ErGPCR-3-GFP sample under DMSO treatment. The homotetramer (~380 kDa) was induced in the ErGPCR-3-GFP samples after 20E treatment. ErGPCR-3$^{\Delta C-terminal}$-GFP still formed a homotetramer after 20E treatment; however, ErGPCR-3-M-GFP could not form a homotetramer after 20E treatment (Fig. 6D). These results suggest that the 20E binding sites were essential for 20E-triggered formation of the ErGPCR-3 homotetramer.

The role of the ErGPCR-3 homotetramer in the entry of 20E into cells was examined in HaEpi cells and larval tissues. The 20E titer increased in the nuclei of cells when ErGPCR-3 was overexpressed in the cells. Moreover, the 20E titer was even higher after knockdown of *GRK2*, which normally arrests ErGPCR-3 in the cell membrane (Fig. S8), compared with the *dsRFP* control (Fig. 6E). However, the 20E level decreased in the nuclei of cells

overexpressing ErGPCR-3-M-GFP, the binding site mutant, compared with that for ErGPCR-3-GFP under *dsGRK2* and 20E treatment (Fig. 6F), in which conditions ErGPCR-3-M-GFP formed fewer homotetramers (~380 kDa) than ErGPCR-3-GFP (Fig. 6G). These results suggest the ErGPCR-3 homotetramer correlates with 20E entry into cells.

To find evidence that ErGPCR-3 forms a homotetramer *in vivo* and its relationship with the 20E titer in tissues, we examined the wing and midgut at the sixth instar 96 h (wandering stage), at which point the wing is growing and the larval midgut is undergoing remodeling. The 20E titer was higher in the midgut than in the wing disk (Fig. 6H). Consistently, the amount of homotetramer (~240 kDa) was higher in the midgut than that in the wing disk (Fig. 6I), presenting evidence that ErGPCR-3 forms a homotetramer and is related to 20E cell entry *in vivo*.

To understand the physiological significance of controlling the amount of 20E entering cells, the effect of different 20E concentrations on cell fates was examined. The proliferative signal,

p-Histone H3, was detected in 16% of 20E-treated cells using 20E at a final concentration of 0.5 µM, compared with the DMSO-treated cells. In contrast, the p-Histone H3 signal decreased significantly in response to a high concentration 20E (5 µM) compared with the cells treated with DMSO (Fig. S9A,A′). Flow cytometry analysis showed that 0.5 µM 20E did nod induce apoptosis; however, higher concentrations of 20E (2–5 µM) induced apoptosis compared with DMSO treatment (Fig. S9B,B′). These data suggest that low concentrations of 20E promote HaEpi cell proliferation, whereas high concentrations promote apoptosis.

DISCUSSION

Several GPCRs are proposed to transmit steroid hormone signaling as cell membrane receptors in mammals and in insects; however, the mechanism is unclear. The present study found that ErGPCR-3 functions as a homotetramer to transmit 20E signal and increase 20E entry into cells (Fig. 7).

20E transmits signal through ErGPCR-3

ErGPCR-3 is the fourth GPCR identified to bind and transmit 20E in *H. armigera*, following ErGPCR-1 (Cai et al., 2014), ErGPCR-2 (Wang et al., 2015) and DopEcR (Kang et al., 2019). Some differences have been observed in these GPCRs, e.g. DopEcR belongs to class A (Rhodopsin-like), whereas ErGPCR-1, ErGPCR-2 and ErGPCR-3 belong to class B (secretin receptor methuselah-2 family, Mth). ErGPCR-1 induces a Ca^{2+}-PKC pathway, whereas ErGPCR-2 and DopEcR induce both GPCR-cAMP-PKA and GPCR-Ca^{2+}-PKC pathways (Jing et al., 2016). ErGPCR-1 does not bind 20E; however, both ErGPCR-2 and DopEcR bind 20E (Kang et al., 2019). ErGPCR-3 also binds 20E to activate both PKA and PKC pathways. These data suggest that several GPCRs could serve as 20E cell membrane receptors by binding 20E, or serve as 20E signal transmitters without binding.

One possible reason that several GPCRs transmit the 20E signal and function as 20E cell membrane receptors is that Mth proteins are believed to have arisen from one ancestral gene and were subsequently duplicated in insects (Li et al., 2013). The physiological significance of their overlapping and/or redundant functions might be explained by the evolutionarily redundant replication of the 20E membrane receptor-related genes. Another reason might be the universally conserved positions in the barcode of G proteins that allow the receptors to bind and activate G proteins in a similar manner. Different receptors recognize the unique positions of the G-protein barcode through distinct residues, such as multiple keys (receptors) with non-identical shapes opening the same lock (G protein) (Flock et al., 2017). One ligand using multiple receptors is common in organisms. For example, in humans adrenaline uses several GPCRs (e.g. α1-adrenoceptors, α2-adrenoceptors and β-adrenoceptors) as its receptors (Alberts, 1993; Goldie et al., 1984; Ruffolo et al., 1995). The question of why many GPCRs are involved in same pathway, redundant or specific, might be understood after we obtain a detailed understanding the different functions of GPCRs.

After transmitting a signal, some GPCRs are internalized to desensitize them (Weinberg and Puthenveedu, 2019). GRKs and β-arrestin play important roles in GPCR internalization (Gurevich and Gurevich, 2019). Most GPCRs are phosphorylated by GRKs and internalized by interacting with β-arrestin (Ritter and Hall, 2009) and clathrin (Kang et al., 2014; Oakley et al., 1999); therefore, GPCRs are inhibited from further interactions with G proteins (Murga et al., 2019). ErGPCR-3 desensitization depends on a similar mechanism. This characteristic is quite similar to ErGPCR-2 (Wang et al., 2015), but different from either ErGPCR-1, which is desensitized by β-arrestin-1 binding without endocytosis (Zhang et al., 2015), and DopEcR, which is not internalized (Kang et al., 2019).

ErGPCR-3 functions as a homotetramer

Class A and class B GPCRs can transmit signal as a single molecule; however, they are observed to exist as homo- or hetero-
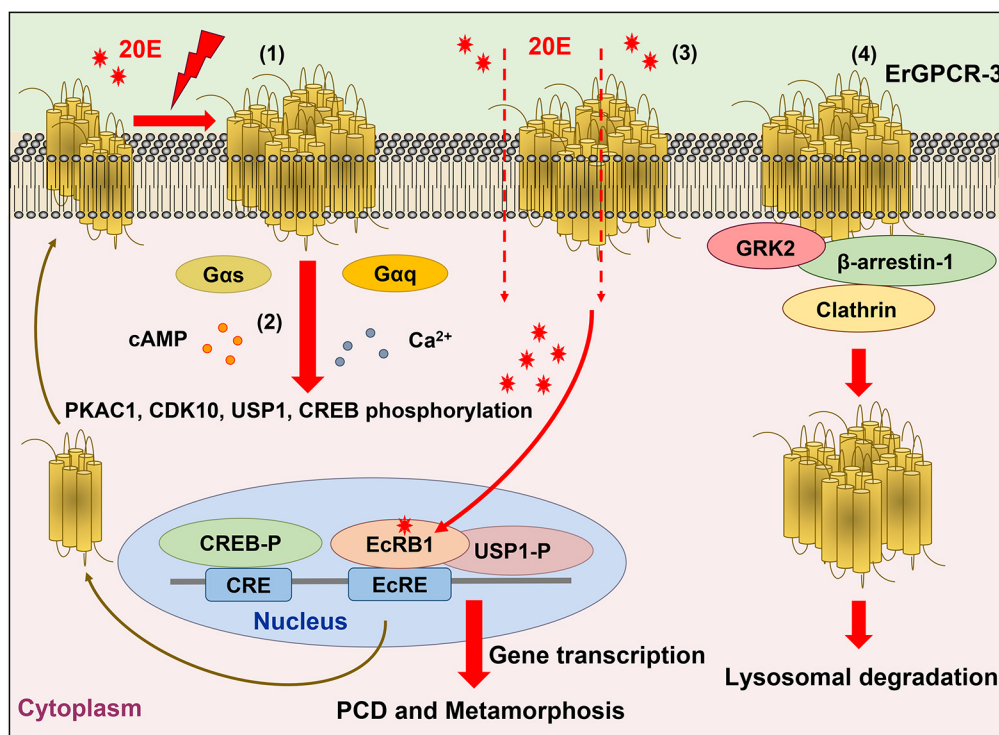
Fig. 7. Proposed mechanism by which ErGPCR-3 transmits the 20E signal and promotes 20E entry into cells. (1) 20E binds to ErGPCR-3 and induces ErGPCR-3 homotetramerization from a constitutive homodimer. (2) ErGPCR-3 interacts with Gαq and Gαs to increase cytosolic calcium and cAMP rapidly, leading to phosphorylation of PKAC1, CDK10, USP1 and CREB to regulate gene expression. (3) ErGPCR-3 homotetramer increases 20E entering the cells to bind to the nuclear receptor EcRB1 to promote gene expression and apoptosis during metamorphosis. (4) ErGPCR-3 homotetramer is internalized by GRK2-mediated phosphorylation and participation of β-arrestin-1 and clathrin, and degraded to desensitize GPCR and terminate the 20E signal. Red asterisks indicate 20E signaling. Red flash indicates the possible ways for 20E to enter cells.

oligomers, and the biological roles of oligomerization are unclear (Gurevich and Gurevich, 2018). Ligand binding is able to induce dimers and oligomers of Class A GPCRs (Milligan et al., 2019). In the present study, we found that ErGPCR-3 forms a constitutive homodimer and is induced to form a homotetramer via 20E binding. This is the first example of a GPCR functioning as a homotetramer in steroid hormone signaling to transmit the signal and increase the cell entry of the hormone.

20E requires a cell membrane transporter, EcI, to enter the receiving cells from circulation, which illustrates that the steroid hormone enters the cell not by simple diffusion, but is facilitated by a transporter (Okamoto et al., 2018). EcI contains 12 transmembrane domains and is thought to transport ecdysone through a single positively charged pore; however, EcI is required for ecdysone import, but not for downstream ecdysteroid signaling (Kalliokoski and Niemi, 2009). Whether a GPCR homotetramer functions as a membrane transporter for 20E or not cannot be proven yet because of technical limitations. ErGPCR-3 signaling might affect the expression and/or subcellular localization of EcI, which in turn promotes 20E entry into the cells. This work presents evidence to support the facilitated diffusion of the steroid hormones in the lepidopteran H. armigera, in addition to the known cell membrane transporter EcI in D. melanogaster. The relationship between ErGPCR-3 and EcI, facilitating diffusion of 20E independently or interactively, is an intriguing question that needs further study.

A low concentration of 20E stimulated rapid cell proliferation in imaginal disks in B. mori (Koyama et al., 2004), and a high titer of 20E suppressed proliferation in imaginal disks and caused cessation of growth in peripheral tissues (Edgar, 2006). A high 20E concentration (5 μM) is necessary to initiate apoptosis in H. armigera by triggering activation of caspase-3 via increasing the calcium level and the cleavage of autophagy-related gene 5 (ATG5) (Li et al., 2016). The 20E titer varies from 0.1 μM during larval growth to over 9 μM during metamorphosis in H. armigera (Di et al., 2020; Kang et al., 2019). The 20E titer is similarly high in the hemolymph during metamorphosis; however, the wing disk is proliferating, and the larval midgut is experiencing programmed cell death (PCD) during this stage. Our results suggest a GPCR-mediated mechanism of 20E cell entry, which provides important implications for controlling wing disk and midgut development during metamorphosis.

MATERIALS AND METHODS
Insects and cells
Cotton bollworms (H. armigera) were reared in our laboratory on an artificial diet (Zhao et al., 1998) at 27°C under a 14 h light/10 h dark photoperiod and 40-50% relative humidity. HaEpi (Shao et al., 2008) was established and maintained at 27°C in Grace's medium supplemented with 10% fetal bovine serum (FBS; Invitrogen). The Sf9 cell line (Thermo Fisher Scientific) was cultured in ESF921 medium (Expression Systems) at 27°C without any serum or additives, unless mentioned. All cultured cells were monitored regularly for bacteria and mycoplasma contamination.

ErGPCR-3 screening and bioinformatic analysis
GPCRs were identified from the transcriptome of HaEpi cells treated with 2 μM 20E (Sigma-Aldrich) for 12 h. The mRNA levels of GPCRs in larvae were examined using qRT-PCR after injection of 20E or dsRNA, with an equal amount of diluted DMSO as a solvent control. The functional domains and motifs of the obtained proteins were predicted using SMART (http://smart.embl-heidelberg.de/). The molecular characterization of proteins was performed using the ExPASy ProtParam tool (https://web.expasy.org/protparam/). Multiple amino acid sequence alignment was performed using ClustalX and phylogenetic trees were constructed using the Neighbor-Joining (NJ) method in MEGA 7.0. The ligand binding site predictions of ErGPCR-3 were simulated using I-TASSER COACH (https://zhanglab.

ccmb.med.umich.edu/COACH/) and PyMOL-v1.7 was used to visualize the three-dimensional structure and to label important structural features.

20E induction in larvae
20E powder was dissolved in DMSO from the stock solution at 20 mM and diluted in phosphate-buffered saline (PBS) [140 mM NaCl, 10 mM sodium phosphate (pH 7.4)] when needed. 20E was injected into the sixth instar 6 h larval hemocoel. An equal amount of diluted DMSO was used as a control.

RNA interference in larvae and cells
The detailed method for H. armigera dsRNA synthesis was described in a previous report (Chen et al., 2017). DNA fragments – 5′-649 bp-1102 bp-3′ of ErGPCR-3, 5′-691 bp-1205 bp-3′ of USP1 (EU526832.1), 5′-127 bp-474 bp-3′ of EcRB1 (EU526831.1), 5′-1093 bp-1636 bp-3′ of GRK2 (KT364485.1) and 5′-740 bp-1171 bp-3′ of β-arrestin-1 (KP027422.1) – were amplified as the template for dsRNA synthesis using the primers RNAiF and RNAiR, which incorporated the T7 promoter (Table S1). The dsRNA was synthesized according to the method described in the MEGAscript RNAi Kit (Ambion). The phenol-chloroform method was used to purify the dsRNA. The purity and integrity of the dsRNA were examined using agarose gel electrophoresis, and then quantified using microvolume spectrophotometers (GeneQuant; Amersham Biosciences). The dsRNA for ErGPCR-3 was injected into the sixth instar larval hemocoel from the side of the front abdomen three times at 6, 24 and 48 h using a micro-syringe. Each injection comprised 500 ng/larva of dsRNA. The dsGFP was used as a control. After the third dsRNA injection, 500 ng of 20E/larva was injected into the larval hemocoel. An equal amount of DMSO was injected as a control. Thirty larvae were injected for each treatment and three independent biological replicates were performed. The phenotypes and developmental rates of the individuals were recorded daily. Total RNA and protein were extracted to verify the effects of RNAi 2 days after 20E injection.

HaEpi cells were transfected with dsRNA when the cells were cultured to 70% density. Transfection was performed using the Quick Shuttle-enhanced transfection reagent (Beijing Biodragon Immunotechnologies) according to the manufacturer's instructions. A mixture of 2 μg of dsRNA and 5 μl of transfection reagent was transfected into the cells in 1 ml of Grace's medium. The equivalent amount of dsGFP was used as the control. 20E at 2 μM was added to the Grace's medium for 6 h after 48 h of dsRNA transfection. The controls were treated with the equivalent volume of DMSO. Total RNA was then isolated and reverse-transcribed for qRT-PCR analysis. For the qRT-PCR analysis, ACTB (encoding β-actin) was used as a control to normalize the gene expression and the data were analyzed from three biological experiments using the $2^{-\Delta\Delta Ct}$ method: $2^{-\Delta\Delta Ct}=2^{-[(CTtreat\ of\ gene-CTtreat\ of\ ACTB)-(CTcon\ of\ gene-CTcon\ of\ ACTB)]}$ where CTcon is the cycle threshold (CT) value of the control group and CTtreat was the CT value of the experimental group.

Preparation of the antiserum against ErGPCR-3
A fragment encoding a portion of ErGPCR-3 (amino acids 82-621) was amplified using primers ErGPCR-3ExpF and ErGPCR-3ExpR (Table S1). The PCR product was inserted into the pET-32a(+) expression vector (Promega) to produce the recombinant protein in Escherichia coli rosette cells by 0.1 mM isopropyl β-D-thiogalactoside (IPTG) induction. The target protein was purified using an Ni^{2+}-NTA affinity column (GE Healthcare). Then, 500 μg of the purified recombinant protein (in 1 ml) and 1 ml of complete Freund's adjuvant (Sigma-Aldrich) were mixed completely and injected subcutaneously into a rabbit's back. Three weeks later, 500 μg of purified recombinant protein was mixed with 1 ml of incomplete Freund's adjuvant (Sigma-Aldrich) and injected into the same rabbit according to the previous method. Then, 500 μg of purified protein was directly injected into the leg muscles of the same rabbit after an additional 2 weeks. The serum was collected after two weeks, and the specificity of the antiserum was determined using western blotting via RNAi (Fig. S4E).

Western blotting
Total proteins were extracted from cells or larval tissues using PBS supplemented with 1 mM PMSF, followed by centrifugation at 10,000 g at 4°C for 10 min. The protein concentration was determined using Bradford's

method (Bradford, 1976). Total proteins (20 µg) from each sample were subjected to 7.5-12.5% SDS-PAGE and then electrophoretically transferred onto a nitrocellulose membrane. The membrane was incubated with blocking buffer containing 5% skim milk in Tris-buffered saline [TBS; 10 mM Tris-HCl and 150 mM NaCl (pH 7.5)] for 1 h at room temperature and then incubated at 4°C overnight with the primary antibodies diluted 1:100 for rabbit polyclonal antibodies or 1:1000 for mouse monoclonal antibodies in blocking buffer. Rabbit polyclonal antibodies against *H. armigera* ErGPCR-3 were produced in our laboratory. Rabbit polyclonal antibodies against β-actin and mouse monoclonal antibodies against His, GFP, and RFP were purchased from ABclonal (AC026, AE003, AE012, and AE020). Antibodies were diluted in 5% bovine serum albumin (BSA) at 1:5000-1:10,000. The nitrocellulose membrane was washed three times for 10 min each with TBST (0.02% Tween in TBS), followed by incubation for 2 h at room temperature with the alkaline phosphatase-labeled goat anti-rabbit or anti-mouse IgG secondary antibodies (Sangon, D110072 and D110089, respectively) diluted 1:5000 in blocking buffer. The membrane was washed three times for 10 min each with TBST and then washed three times for 5 min each with TBS. The target bands were visualized in 10 ml TBS containing 45 µl of 5% *p*-nitro-blue tetrazolium chloride (NBT) and 35 µl 5% 5-bromo-4-chloro-3-indolyl phosphate (BCIP) in the dark for 10 min. The densities of the bands on the western blotting were acquired using ImageJ software (National Institutes of Health, http//imagej.nih.gov/ij/download.html).

H&E staining
The larval midgut or fat body was isolated and fixed with PBS containing 4% paraformaldehyde at 4°C overnight. The fixed tissues were dehydrated gradually. The tissues were then embedded in melted paraffin and sliced into 7-µm sections using a paraffin-slicing machine (Leica RM2245). The sections were adhered to gelatin-coated glass slides immediately. The slides were dried at 42°C overnight and subsequently dewaxed. The midgut sections were rehydrated gradually and digested with 20 mM proteinase K at 37°C for 10 min. The midgut sections were stained using an H&E staining kit (Sangon) according to the manufacturer's instruction. Positive signals were observed using an Olympus BX51 fluorescence microscope.

Detection of cellular calcium ions
HaEpi cells were transfected with dsRNA for 24 h as previously described. The cells were incubated with 3 µM acetoxymethyl (AM) ester Calcium Crimson™ dye (Invitrogen) in Dulbecco's phosphate-buffered saline (DPBS) [137 mM NaCl, 2.7 mM KCl, 1.5 mM KH$_2$PO$_4$ and 8 mM Na$_2$HPO$_4$ (pH 7.4)] for 30 min at 27°C. The cells were then washed with DPBS three times and exposed to 1 µM 20E in DPBS for 2 min to detect the intracellular calcium release. Next, 1 mM calcium chloride was added to the medium to induce extracellular calcium influx. A laser scanning confocal microscope (Carl Zeiss LSM 700) was used to detect the fluorescence at 555 nm every 6 s for 420 s. The data were analyzed using the Image Pro-Plus software (Media Cybernetics).

cAMP measurements
HaEpi cells were cultured in six-well plates to 70% confluence, and then Grace's insect medium was replaced with DPBS supplemented with 0.5 mM 3-isobutyl-1-methylxanthine (Sigma-Aldrich). After 30 min, the cells were treated with 2 µM 20E for 30 min. DMSO-treated cells served as a solvent control. The medium was removed and the cells were incubated with 500 µl of 0.1 M HCl for 10 min until the cells were completely dissolved. The mixture was centrifuged at room temperature for 5 min at 600 *g*. The supernatant was harvested and the cAMP concentration was measured using a cAMP enzyme-linked immunosorbent assay (ELISA) Kit (Beijing Biodragon Immunotechnologies) according to the manufacturer's instructions.

Overexpression of proteins in HaEpi cells and Co-IP
The open reading frames (ORFs) of genes from *H. armigera* were amplified using the corresponding primers (Table S1) and then inserted into pIEx-4-GFP/RFP-His vector (Invitrogen) fused with green fluorescent protein (GFP) or red fluorescent protein (RFP) through double enzyme digestion to

construct the vector in which the C-terminal of the protein of interest is fused with GFP/RFP and histidine tags. The recombinant vectors were verified via direct DNA sequencing. The reconstructed plasmids were transfected into cells using the QuickShuttle-enhanced transfection reagent (Beijing Biodragon Immunotechnologies) until the cells reached 70-80% confluence. After culturing in Grace's medium supplemented with 10% FBS for 48 h at 27°C, the cells were used in subsequent experiments. The pIEx-4-GFP/RFP-His vector was transfected as a negative control. The overexpressed proteins were detected by western blotting using mouse monoclonal antibody against the corresponding tag (ABClonal, AE012 and AE020, 1:1000). After vectors were transfected into the HaEpi for 48 h, the cells were treated with 2 µM 20E for 1 h, and DMSO was used as the control. Proteins were subsequently extracted using the radioimmunoprecipitation assay (RIPA) buffer [0.1 M Tris-HCl buffer containing 0.2 M NaCl and 1% NP-40 (pH 8)] (Beyotime) with protease and phosphatase inhibitors (Roche Diagnostics) and the supernatant was collected via 4°C centrifugation at 12,000 *g* for 10 min. The supernatant supplemented with protein A resin was incubated with rotation for 5 min at 4°C and collected by centrifugation (1000 *g* for 2 min) to eliminate nonspecific binding. The antibodies were incubated with the supernatant for 4 h at 4°C. The protein A resin was then added to the protein-antibody complex and shaken gently for 2-4 h at 4°C to form the protein-resin-antibody complex. The resin was subsequently collected via centrifugation and washed three times with RIPA buffer. The collected resin was treated with SDS-PAGE loading buffer and boiled for 10 min. The samples were loaded into SDS-PAGE for western blotting using mouse monoclonal antibodies against RFP, GFP, and His (ABClonal) to detect the target proteins, respectively.

Immunocytochemistry
HaEpi cells grown on cover slips in a cell culture plate were washed with PBS twice and fixed with PBS containing 4% paraformaldehyde in the dark for 10 min. The plasma membrane was stained with WGA (Sigma-Aldrich; 1 µg/ml in PBS) in the dark for 5 min and then washed with PBS three times. The midgut sections and the fixed cells were blocked with 2% BSA in PBS for 1 h and then incubated with rabbit polyclonal antibodies against ErGPCR-3 as the primary antibody (1:100 dilution in 2% BSA) overnight at 4°C. The midgut sections and the cells were washed and subsequently incubated with Alexa Fluor 488-labeled goat anti-rabbit IgG secondary antibodies (diluted 1:1000 in 2% BSA) for 1 h at 37°C. Nuclei were stained with 4′,6-diamidino-2-phenylindole (DAPI; Sangon; 1 µg/ml in PBS) in the dark for 10 min and then washed with PBS three times. Fluorescence was detected using a laser scanning confocal microscope (Carl Zeiss, LSM 700).

Structure modeling and ligand docking of ErGPCR-3
The molecular model of ErGPCR-3 binding to a steroid was created using the I-TASSER server (https://zhanglab.ccmb.med.umich.edu/I-TASSER/). The ligand 20E was docked into the active site of ErGPCR-3 using the Surflex-Dock (SFXC) function in the SYBYLx2.0 software (Tripos). Figures were prepared using the PyMOL program (Seeliger and de Groot, 2010).

Detecting 20E bound by the cell membranes of HaEpi cells and the saturation binding curve of GPCRs to 20E
pIEx-4-GFP-His, pIEx-4-ErGPCR-3-GFP-His and the ErGPCR-3 mutant [pIEx-4-ErGPCR-3-M-GFP-His: leucine 449 to alanine (L449A), leucine 474 to alanine (L474A), glycine 662 to alanine (G662A), and leucine 669 to alanine (L669A)], which was obtained by site-directed mutagenesis of ErGPCR-3 on possible steroid binding sites (Table S2) based on the I-TASSER prediction, were transfected into HaEpi cells, separately. The detailed method of detecting 20E bound by the cell membranes of HaEpi cells has been previously reported (Kang et al., 2019). GPCRs-GFP-His and GFP-His were overexpressed in Sf9 cells and isolated, and then a 20E-EIA kit was used for binding saturation curve analysis, according to a previously published method (Kang et al., 2019).

Detecting the 20E titer in tissues and cells
Midguts and wing disks (10 mg) were dissected from around five larvae of sixth instar 96 h and then freeze-dried overnight. The powders were

dissolved in 200 µl of 80% methyl alcohol and ground in a cold mortar. After centrifugation at 10,000 g for 10 min, the supernatant was air dried at room temperature. The precipitates were completely dissolved with 100 µl of EIA buffer. Each sample was diluted 1000 times with EIA buffer before detection of the 20E concentration. A 50 µl sample was used to detect 20E using a 20E-EIA kit according to a previously published method (Kang et al., 2019).

dsGRK2 and *dsErGPCR-3* were transfected into HaEpi cells in a six-well cell culture plate for 48 h. *dsRFP* was the control. pIEx-4-ErGPCR-3-GFP-His or pIEx-4-ErGPCR-M-3-GFP-His and *dsGRK2* were co-transfected into HaEpi cells in a 25-cm^2 cell culture bottle for 48 h. pIEx-4-GFP-His and *dsRFP* were used as the control. 20E was then added to the medium at 2 µM and incubated for 30 min at 27°C. To detect the intracellular 20E, the nuclei of cells were isolated using a Nuclear and Cytoplasmic Protein Extraction Kit (Beyotime) and then freeze-dried overnight. The powders were dissolved in 200 µl of 80% methyl alcohol and ground in a cold mortar. After centrifugation at 10,000 g for 10 min, the supernatant was air dried at room temperature. The precipitates were completely dissolved with 100 µl of EIA buffer. The intracellular 20E levels were detected using the 20E-EIA kit according to a previously published method (Kang et al., 2019).

Oligomerization determination

BS3 (Sigma Aldrich) possesses a charged group and is used to cross-link cell surface proteins (Angers et al., 2000; Friedrichson and Kurzchalia, 1998). The assay was performed according to the manufacturer's protocol. HaEpi cells and tissues were collected and washed three times with ice-cold DPBS and then incubated with DPBS containing 1 µM 20E or the equivalent concentration of DMSO. The resuspended HaEpi cells and the tissue homogenates were incubated with 5 mM BS3 and the reaction mixture was incubated at room temperature for 1 h. Tris-HCl (pH 7.5) was then added into the mixture at a final concentration of 20 mM to quench the crosslinking reaction. The crosslinking-treated HaEpi cells and the tissue homogenates were homogenized and subjected to western blotting.

Detection of cell proliferation and apoptosis

HaEpi cells were treated with 0.5-5 µM 20E for 48 or 72 h. DMSO was used as a control. The p-Histone H3 (Ser10) antibody (rabbit polyclonal antibodies, 9701, Cell Signaling Technology, 1:1000 dilution in 2% BSA) was used to detect cell proliferation. The nuclei were stained with DAPI (10 µg/ml) for 10 min at room temperature in the dark, and observed using a laser scanning confocal microscope (Carl Zeiss, LSM 700). Annexin-V and propidium iodide (PI) were used to detect cell apoptosis using an Annexin V-FITC Apoptosis Detection kit (GK3603, Genview) and flow cytometry (Amnis). Annexin V-FITC stained the earlier apoptotic cells by binding to the membrane phosphatidylserine, and PI indicated the later apoptotic cells and dead cells by entering the cells.

Statistical analyses

The experimental data were analyzed using SPSS 23.0 (IBM) and generated using GraphPad Prism 5. All data are mean±standard deviation (s.d.) of at least three biologically independent experiments. Two group datasets were analyzed using two-tailed Student's t-test, $*P<0.05$, $**P<0.01$, $***P<0.001$. One-way ANOVA was used to analyze the differences among three or more groups using Duncan's multiple comparison test at $P=0.05$.

References

Alberts, P. (1993). Subtype classification of presynaptic α₂-adrenoceptors. *Gen. Pharmacol. Vasc. Syst.* **24**, 1-8. doi:10.1016/0306-3623(93)90003-G

Angers, S., Salahpour, A., Joly, E., Hilairet, S., Chelsky, D., Dennis, M. and Bouvier, M. (2000). Detection of beta 2-adrenergic receptor dimerization in living cells using bioluminescence resonance energy transfer (BRET). *Proc. Natl. Acad. Sci. USA* **97**, 3684-3689. doi:10.1073/pnas.060590697

Benovic, J. L., DeBlasi, A., Stone, W. C., Caron, M. G. and Lefkowitz, R. J. (1989). Beta-adrenergic receptor kinase: primary structure delineates a multigene family. *Science* **246**, 235-240. doi:10.1126/science.2552582

Bhattacharyya, S., Warfield, K. L., Ruthel, G., Bavari, S., Aman, M. J. and Hope, T. J. (2010). Ebola virus uses clathrin-mediated endocytosis as an entry pathway. *Virology* **401**, 18-28. doi:10.1016/j.virol.2010.02.015

Bockaert, J. and Pin, J. P. (1999). Molecular tinkering of G protein-coupled receptors: an evolutionary success. *EMBO J.* **18**, 1723-1729. doi:10.1093/emboj/18.7.1723

Bradford, M. M. (1976). A rapid and sensitive method for the quantitation of microgram quantities of protein utilizing the principle of protein-dye binding. *Anal. Biochem.* **72**, 248-254. doi:10.1016/0003-2697(76)90527-3

Cai, M.-J., Dong, D.-J., Wang, Y., Liu, P.-C., Liu, W., Wang, J.-X. and Zhao, X.-F. (2014). G-protein-coupled receptor participates in 20-hydroxyecdysone signaling on the plasma membrane. *Cell Commun. Signal.* **12**, 9. doi:10.1186/1478-811X-12-9

Chen, X., Zheng, C., Qian, J., Sutton, S. W., Wang, Z., Lv, J., Liu, C. and Zhou, N. (2014). Involvement of β-arrestin-2 and clathrin in agonist-mediated internalization of the human cannabinoid CB2 receptor. *Curr. Mol. Pharmacol.* **7**, 67-80. doi:10.2174/1874467207666140714115824

Chen, C. H., Pan, J., Di, Y. Q., Liu, W., Hou, L., Wang, J. X. and Zhao, X. F. (2017). Protein kinase C delta phosphorylates ecdysone receptor B1 to promote gene expression and apoptosis under 20-hydroxyecdysone regulation. *Proc. Natl. Acad. Sci. USA* **114**, E7121-E7130. doi:10.1073/pnas.1704999114

Cheng, Z.-J. and Miller, L. J. (2001). Agonist-dependent dissociation of oligomeric complexes of G protein-coupled cholecystokinin receptors demonstrated in living cells using bioluminescence resonance energy transfer. *J. Biol. Chem.* **276**, 48040-48047. doi:10.1074/jbc.M105668200

Cheng, Z.-J., Harikumar, K. G., Holicky, E. L. and Miller, L. J. (2003). Heterodimerization of type A and B cholecystokinin receptors enhance signaling and promote cell growth. *J. Biol. Chem.* **278**, 52972-52979. doi:10.1074/jbc.M310090200

Dahlman-Wright, K., Cavailles, V., Fuqua, S. A., Jordan, V. C., Katzenellenbogen, J. A., Korach, K. S., Maggi, A., Muramatsu, M., Parker, M. G. and Gustafsson, J.-A. (2006). International union of pharmacology. LXIV. Estrogen receptors. *Pharmacol. Rev.* **58**, 773-781. doi:10.1124/pr.58.4.8

Di, Y.-Q., Han, X.-L., Kang, X.-L., Wang, D., Chen, C.-H., Wang, J.-X. and Zhao, X.-F. (2020). Autophagy triggers CTSD (cathepsin D) maturation and localization inside cells to promote apoptosis. *Autophagy* [Epub ahead of print]. doi:10.1080/15548627.2020.1752497

Ding, W. Q., Cheng, Z. J., McElhiney, J., Kuntz, S. M. and Miller, L. J. (2002). Silencing of secretin receptor function by dimerization with a misspliced variant secretin receptor in ductal pancreatic adenocarcinoma. *Cancer Res.* **62**, 5223-5229.

Edgar, B. A. (2006). How flies get their size: genetics meets physiology. *Nat. Rev. Genet.* **7**, 907-916. doi:10.1038/nrg1989

Flock, T., Hauser, A. S., Lund, N., Gloriam, D. E., Balaji, S. and Babu, M. M. (2017). Selectivity determinants of GPCR-G-protein binding. *Nature* **545**, 317-322. doi:10.1038/nature22070

Friedrichson, T. and Kurzchalia, T. V. (1998). Microdomains of GPI-anchored proteins in living cells revealed by crosslinking. *Nature* **394**, 802-805. doi:10.1038/29570

Goldie, R. G., Paterson, J. W., Spina, D. and Wale, J. L. (1984). Classification of β-adrenoceptors in human isolated bronchus. *Brit. J. Pharmacol.* **81**, 611-615. doi:10.1111/j.1476-5381.1984.tb16125.x

Gonzalez-Noriega, A., Grubb, J. H., Talkad, V. and Sly, W. S. (1980). Chloroquine inhibits lysosomal enzyme pinocytosis and enhances lysosomal enzyme secretion by impairing receptor recycling. *J. Cell Biol.* **85**, 839-852. doi:10.1083/jcb.85.3.839

Gorski, J. and Gannon, F. (1976). Current models of steroid hormone action: a critique. *Annu. Rev. Physiol.* **38**, 425-450. doi:10.1146/annurev.ph.38.030176.002233

DEVELOPMENT

Gurevich, V. V. and Gurevich, E. V. (2018). GPCRs and signal transducers: interaction stoichiometry. *Trends Pharmacol. Sci.* **39**, 672-684. doi:10.1016/j.tips.2018.04.002

Gurevich, V. V. and Gurevich, E. V. (2019). GPCR signaling regulation: the role of GRKs and Arrestins. *Front. Pharmacol.* **10**, 125. doi:10.3389/fphar.2019.00125

He, Y., Gao, X., Goswami, D., Hou, L., Pal, K., Yin, Y., Zhao, G., Ernst, O. P., Griffin, P., Melcher, K., et al. (2017). Molecular assembly of rhodopsin with G protein-coupled receptor kinases. *Cell Res.* **27**, 728-747. doi:10.1038/cr.2017.72

Jing, Y.-P., Wang, D., Han, X.-L., Dong, D.-J., Wang, J.-X. and Zhao, X.-F. (2016). The steroid hormone 20-hydroxyecdysone enhances gene transcription through the cAMP response element-binding protein (CREB) signaling pathway. *J. Biol. Chem.* **291**, 12771-12785. doi:10.1074/jbc.M115.706028

Kalliokoski, A. and Niemi, M. (2009). Impact of OATP transporters on pharmacokinetics. *Brit. J. Pharmacol.* **158**, 693-705. doi:10.1111/j.1476-5381.2009.00430.x

Kang, D. S., Tian, X. and Benovic, J. L. (2014). Role of β-arrestins and arrestin domain-containing proteins in G protein-coupled receptor trafficking. *Curr. Opin. Cell Biol.* **27**, 63-71. doi:10.1016/j.ceb.2013.11.005

Kang, X.-L., Zhang, J.-Y., Wang, D., Zhao, Y.-M., Han, X.-L., Wang, J.-X. and Zhao, X.-F. (2019). The steroid hormone 20-hydroxyecdysone binds to dopamine receptor to repress lepidopteran insect feeding and promote pupation. *PLoS Genet.* **15**, e1008331. doi:10.1371/journal.pgen.1008331

Koyama, T., Iwami, M. and Sakurai, S. (2004). Ecdysteroid control of cell cycle and cellular commitment in insect wing imaginal discs. *Mol. Cell. Endocrinol.* **213**, 155-166. doi:10.1016/j.mce.2003.10.063

Kroeger, K. M., Hanyaloglu, A. C., Seeber, R. M., Miles, L. E. C. and Eidne, K. A. (2001). Constitutive and agonist-dependent homo-oligomerization of the thyrotropin-releasing hormone receptor. Detection in living cells using bioluminescence resonance energy transfer. *J. Biol. Chem.* **276**, 12736-12743. doi:10.1074/jbc.M011311200

Li, C., Chen, M., Sang, M., Liu, X., Wu, W. and Li, B. (2013). Comparative genomic analysis and evolution of family-B G protein-coupled receptors from six model insect species. *Gene* **519**, 1-12. doi:10.1016/j.gene.2013.01.061

Li, Y.-B., Li, X.-R., Yang, T., Wang, J.-X. and Zhao, X.-F. (2016). The steroid hormone 20-hydroxyecdysone promotes switching from autophagy to apoptosis by increasing intracellular calcium levels. *Insect Biochem. Mol. Biol.* **79**, 73-86. doi:10.1016/j.ibmb.2016.10.004

Liu, W., Cai, M.-J., Wang, J.-X. and Zhao, X.-F. (2014a). In a nongenomic action, steroid hormone 20-hydroxyecdysone induces phosphorylation of cyclin-dependent kinase 10 to promote gene transcription. *Endocrinology* **155**, 1738-1750. doi:10.1210/en.2013-2020

Liu, W., Cai, M.-J., Zheng, C.-C., Wang, J.-X. and Zhao, X.-F. (2014b). Phospholipase Cγ1 connects the cell membrane pathway to the nuclear receptor pathway in insect steroid hormone signaling. *J. Biol. Chem.* **289**, 13026-13041. doi:10.1074/jbc.M113.547018

Lohse, M. J., Benovic, J. L., Codina, J., Caron, M. G. and Lefkowitz, R. J. (1990). beta-Arrestin: a protein that regulates beta-adrenergic receptor function. *Science* **248**, 1547-1550. doi:10.1126/science.2163110

Manaboon, M., Iga, M., Iwami, M. and Sakurai, S. (2009). Intracellular mobilization of Ca^{2+} by the insect steroid hormone 20-hydroxyecdysone during programmed cell death in silkworm anterior silk glands. *J. Insect Physiol.* **55**, 123-129. doi:10.1016/j.jinsphys.2008.10.013

Marinissen, M. J. and Gutkind, J. S. (2001). G-protein-coupled receptors and signaling networks: emerging paradigms. *Trends Pharmacol. Sci.* **22**, 368-376. doi:10.1016/S0165-6147(00)01678-3

Milgrom, E., Atger, M. and Baulieu, E.-E. (1973). Studies on estrogen entry into uterine cells and on estradiol-receptor complex attachment to the nucleus — is the entry of estrogen into uterine cells a protein-mediated process? *Biochim Biophys Acta (BBA) Gen. Subj.* **320**, 267-283. doi:10.1016/0304-4165(73)90307-3

Milligan, G., Ward, R. J. and Marsango, S. (2019). GPCR homo-oligomerization. *Curr. Opin. Cell Biol.* **57**, 40-47. doi:10.1016/j.ceb.2018.10.007

Murga, C., Arcones, A. C., Cruces-Sande, M., Briones, A. M., Salaices, M. and Mayor, F. Jr. (2019). G protein-coupled receptor kinase 2 (GRK2) as a potential therapeutic target in cardiovascular and metabolic diseases. *Front. Pharmacol.* **10**, 112. doi:10.3389/fphar.2019.00112

Oakley, R. H., Laporte, S. A., Holt, J. A., Barak, L. S. and Caron, M. G. (1999). Association of β-arrestin with G protein-coupled receptors during clathrin-mediated endocytosis dictates the profile of receptor resensitization. *J. Biol. Chem.* **274**, 32248-32257. doi:10.1074/jbc.274.45.32248

Okamoto, N., Viswanatha, R., Bittar, R., Li, Z., Haga-Yamanaka, S., Perrimon, N. and Yamanaka, N. (2018). A membrane transporter is required for steroid hormone uptake in *Drosophila*. *Dev. Cell* **47**, 294-305.e7. doi:10.1016/j.devcel.2018.09.012

Pfleger, K. D. G. and Eidne, K. A. (2005). Monitoring the formation of dynamic G-protein-coupled receptor-protein complexes in living cells. *Biochem. J.* **385**, 625-637. doi:10.1042/BJ20041361

Pietras, R. J. and Szego, C. M. (1977). Specific binding sites for oestrogen at the outer surfaces of isolated endometrial cells. *Nature* **265**, 69-72. doi:10.1038/265069a0

Plagemann, P. G. W. and Erbe, J. (1976). Glucocorticoids—uptake by simple diffusion by cultured Reuber and Novikoff rat hepatoma cells. *Biochem. Pharmacol.* **25**, 1489-1494. doi:10.1016/0006-2952(76)90066-6

Revankar, C. M., Cimino, D. F., Sklar, L. A., Arterburn, J. B. and Prossnitz, E. R. (2005). A transmembrane intracellular estrogen receptor mediates rapid cell signaling. *Science* **307**, 1625-1630. doi:10.1126/science.1106943

Riddiford, L. M., Cherbas, P. and Truman, J. W. (2000). Ecdysone receptors and their biological actions. *Vitam. Horm.* **60**, 1-73. doi:10.1016/S0083-6729(00)60016-X

Ritter, S. L. and Hall, R. A. (2009). Fine-tuning of GPCR activity by receptor-interacting proteins. *Nat. Rev. Mol. Cell Biol.* **10**, 819-830. doi:10.1038/nrm2803

Ruffolo, R. R., Jr., Bondinell, W., Ku, T., Naselsky, D. P. and Hieble, J. P. (1995). Alpha 1-adrenoceptors: pharmacological classification and newer therapeutic applications. *Proc. West Pharmacol. Soc.* **38**, 121-126.

Sargiacomo, M., Scherer, P. E., Tang, Z., Kübler, E., Song, K. S., Sanders, M. C. and Lisanti, M. P. (1995). Oligomeric structure of caveolin: implications for caveolae membrane organization. *Proc. Natl. Acad. Sci. USA* **92**, 9407-9411. doi:10.1073/pnas.92.20.9407

Seeliger, D. and de Groot, B. L. (2010). Ligand docking and binding site analysis with PyMOL and Autodock/Vina. *J. Comput. Aided Mol. Des.* **24**, 417-422. doi:10.1007/s10822-010-9352-6

Shao, H.-L., Zheng, W.-W., Liu, P.-C., Wang, Q., Wang, J.-X. and Zhao, X.-F. (2008). Establishment of a new cell line from lepidopteran epidermis and hormonal regulation on the genes. *PLoS ONE* **3**, e3127. doi:10.1371/journal.pone.0003127

Srivastava, D. P., Yu, E. J., Kennedy, K., Chatwin, H., Reale, V., Hamon, M., Smith, T. and Evans, P. D. (2005). Rapid, nongenomic responses to ecdysteroids and catecholamines mediated by a novel *Drosophila* G-protein-coupled receptor. *J. Neurosci.* **25**, 6145-6155. doi:10.1523/JNEUROSCI.1005-05.2005

Wang, D., Zhao, W.-L., Cai, M.-J., Wang, J.-X. and Zhao, X.-F. (2015). G-protein-coupled receptor controls steroid hormone signaling in cell membrane. *Sci. Rep.* **5**, 8675. doi:10.1038/srep08675

Weinberg, Z. Y. and Puthenveedu, M. A. (2019). Regulation of G protein-coupled receptor signaling by plasma membrane organization and endocytosis. *Traffic* **20**, 121-129. doi:10.1111/tra.12628

Zhang, X.-Q., Li, X.-R., Ren, J., Li, Y.-B., Cai, M.-J., Wang, J.-X. and Zhao, X.-F. (2015). β-Arrestin1 interacts with G protein-coupled receptor to desensitize signaling of the steroid hormone 20-hydroxyecdysone in the lepidopteran insect *Helicoverpa armigera*. *Cell. Signal.* **27**, 878-886. doi:10.1016/j.cellsig.2015.01.016

Zhao, X.-F., Wang, J.-X. and Wang, Y.-C. (1998). Purification and characterization of a cysteine proteinase from eggs of the cotton boll worm, *Helicoverpa armigera*. *Insect Biochem. Mol.* **28**, 259-264. doi:10.1016/S0965-1748(98)00015-0